Earth and Space Science

Key Points:

- Electric field experiments require calibration of the shorting factor, a parameter that converts measurements into actual electric field
- We present a method to determine the shorting factors of the Van Allen Probes double-probe electric field instruments near perigee
- Uncertainty in individual electric drift measurements due to uncertainty in the value of the shorting factor is smaller than 10 m/s

Correspondence to:
S. Lejosne,
solene@berkeley.edu

Shorting Factor In-Flight Calibration for the Van Allen Probes DC Electric Field Measurements in the Earth's Plasmasphere

Solène Lejosne[1] [ID] **and F. S. Mozer[1]** [ID]

[1]Space Sciences Laboratory, University of California, Berkeley, CA, USA

Abstract Satellite-based direct electric field measurements deliver crucial information for space science studies. Yet they require meticulous design and calibration. In-flight calibration of double-probe instruments is usually presented in the most common case of tenuous plasmas, where the presence of an electrostatic structure surrounding the charged spacecraft alters the geophysical electric field measurements. To account for this effect and the uncertainty in the boom length, the measured electric field is multiplied by a parameter called the shorting factor (s_f). In the plasmasphere, the Debye length is very small in comparison with spacecraft dimension, and there is no shorting of the electric field measurements ($s_f = 1$). However, the electric field induced by spacecraft motion greatly exceeds any geophysical electric field of interest in the plasmasphere. Thus, the highest level of accuracy in calibration is required. The objective of this work is to discuss the accuracy of the setting $s_f = 1$ and therefore to examine the accuracy of Van Allen Probes electric field measurements below L = 2. We introduce a method to determine the shorting factor near perigee. It relies on the idea that the value of the geophysical electric field measured in the Earth's rotating frame of reference is independent of whether the spacecraft is approaching perigee or past perigee, that is, it is independent of spacecraft velocity. We obtain that $s_f = 0.994 \pm 0.001$. The resulting margins of errors in individual electric drift measurements are of the order of $\pm 0.1\%$ of spacecraft velocity (a few meters per second).

Plain Language Summary Large-scale electric fields are naturally present in space. They are key to understanding plasma dynamics. Yet they are notoriously difficult to measure directly. In situ electric field measurements are especially challenging very close to Earth, when spacecraft pass through perigee with maximum velocity in a strong magnetic field. The field instruments onboard the Van Allen Probes are the first to be accurate enough to measure the geophysical electric field around magnetic equator, even below 3 Earth radii. In this work, we introduce a method to calibrate the data and to determine the margins of errors for the Van Allen Probes electric drift measurements in the Earth's plasmasphere. The corresponding margins of errors are remarkably small (<10 m/s for each individual electric drift measurement). Therefore, this work further demonstrates the ability of Van Allen Probes instruments to resolve small variations in the geophysical electric drift, even very close to Earth. It is the first time that the calibration of near perigee DC electric field measurements is discussed. Such method could potentially be transposed to other missions and other sets of satellite-based electric field measurements to further advance our understanding of transport and energization in space plasmas.

1. Introduction

Double-probe instruments are the most popular way to perform direct measurements of low frequency and direct-current (DC) electric fields in space plasmas. Double probes have flown on a number of rockets, balloons, and satellites, including the S3-3 satellite (Mozer et al., 1977), the Combined Release and Radiation Effects Satellite (Wygant et al., 1992), the Cluster spacecraft (Gustafsson et al., 1997), the Fast Auroral Snapshot Explorer (Ergun et al., 2001), the Time History of Events and Macroscale Interactions during Substorms mission (Bonnell et al., 2008), the Van Allen Probes (Wygant et al., 2013), and the Magnetospheric Multiscale Mission (Lindqvist et al., 2016).

The double-probe technique consists of inferring the geophysical electric field by measuring the potential difference between two separated conductors located at opposite ends of long wire booms and dividing the potential difference by the distance between the conductors. The long wire booms are held straight by

the centrifugal forces in the spacecraft spin plane. The validity and the accuracy of these measurements require meticulous care and sustained attention during mission design, instrument design, data collection, and data analysis (e.g., Mozer, 2016).

In-flight calibration of DC and low-frequency electric field measurements is usually discussed in the case of tenuous plasmas, because spacecraft mostly operate in this condition. Different problems alter or even completely prevent electric field measurements in tenuous magnetospheric plasmas, where the electron density can be as low as $10^4 - 10^5$ m^{-3} (e.g., Engwall et al., 2006; Mozer, 2016; Pedersen et al., 1998). In particular, the electrostatic structure associated with the spacecraft, and the long wire booms interfere with the ambient geophysical electric field (Fahleson, 1967; Mozer et al., 1978). To tackle this difficulty, electric field measurements are multiplied by a parameter called the shorting factor (s_f). This coefficient depends on a multitude of parameters such as spacecraft boom length, geometry of the surfaces near the contact sphere, and Debye length.

Shorting factors ranging from approximately 0.5 to 2 have been derived for different missions. The estimates were based on numerical simulations (e.g., Cully et al., 2007) and/or empirical comparisons between direct electric field measurements and theoretical or experimental estimates (e.g., Califf & Cully, 2016; Khotyaintsev et al., 2014; Pedersen et al., 1984). As plasma density increases and the Debye length decreases, the amplitude of the shorting factor should approach 1 ($s_f = 1$ if the boom length is accurately known).

The electric field measured by the double-probe instrument is in the reference frame moving with the spacecraft. However, the electric field induced by spacecraft motion in the ambient magnetic field is noninteresting in itself. It needs to be subtracted from the raw electric field measurement to estimate the geophysical electric field in a frame of reference fixed to the stars. In the case of the Van Allen Probes, the spacecraft velocity is of the order of 8 km/s around L = 1.4. On the other hand, the geophysical electric drift due to Earth's corotation is of the order of 0.6 km/s close to L = 1.4. This means that more than 90% of the electric field measured is due to spacecraft motion at low L. Most interestingly, the deviations from corotation that are naturally occurring at low L values can be of the order of 100 m/s or less in the Earth's rotating frame of reference (e.g., Richmond et al., 1980). This means that we need to achieve the highest level of accuracy in determining the shorting factor in order to obtain the most accurate in situ measurements of the geophysical DC electric fields naturally present in the Earth's plasmasphere.

The objective of this work is to test the accuracy of the assumption $s_f = 1$ for the Van Allen Probes electric field measurements and to quantify the resulting margins of errors. General results on double-probe DC electric field measurements are introduced in section 2. They show how inaccurate settings of the shorting factor impact empirical estimates of the geophysical electric field. The method to determine Van Allen Probes shorting factors s_f is presented in section 3, together with a discussion of the results.

2. Theoretical Framework for In-Flight Calibration of Near Perigee DC Electric Field Measurements

This section introduces two theoretical results regarding DC electric field measurements. The first result shows how different experimental estimates for the geophysical DC electric field can be obtained when the experimenter postulates different shorting factors. The second result emphasizes the difference that exists between the experimental estimate of the geophysical DC electric field and the true geophysical DC electric field when the shorting factor is not well calibrated. Both formulas will be applied in section 3.

2.1. Relationship Between Measured DC Electric Field, Geophysical DC Electric Field, Spacecraft Motion Induced Electric Field, and True Shorting Factor

The DC electric field measured by a double-probe instrument $\mathbf{E_m}$ multiplied by the appropriate value for the shorting factor $s_{f,i}$ is the sum of (a) the true geophysical DC electric field of interest $\mathbf{E_i}$, in an inertial frame of reference fixed to the stars, and (b) the electric field induced by the spacecraft motion in the ambient magnetic field $\mathbf{B}$ at velocity $\mathbf{V_{sc}}$ (given in the same inertial reference frame):

$$s_{f,i}\mathbf{E_m} = \mathbf{E_i} + \mathbf{V_{sc}} \times \mathbf{B},\tag{1}$$

where $s_{f,i}$ indicates the appropriate (ideal) value for the shorting factor s_f. In practice, the appropriate value for the shorting factor $s_{f,i}$ depends on many parameters. So $s_{f,i}$ is the unknown to determine. The spacecraft velocity $\mathbf{V_{sc}}$ and the ambient magnetic field $\mathbf{B}$ are assumed to be known exactly.

2.2. The Experimental Estimate of the Geophysical Electric Field Depends on the Shorting Factor Value Postulated by the Experimenter

If an experimenter sets a shorting factor value equal to $s_{f,\,exp\,1}$, the geophysical electric field estimated by the first experiment $\mathbf{E_{exp,1}}$ is

$$\mathbf{E_{exp,1}} = s_{f,\,exp1}\mathbf{E_m} - \mathbf{V_{sc}} \times \mathbf{B}.\tag{2}$$

If the shorting factor is set to a different value $s_{f,\,exp\,2}(\neq s_{f,\,exp\,1})$, the electric field obtained in that case $\mathbf{E_{exp,2}}$ is also different ($\mathbf{E_{exp,2}} \neq \mathbf{E_{exp,1}}$):

$$\mathbf{E_{exp,2}} = s_{f,\,exp2}\mathbf{E_m} - \mathbf{V_{sc}} \times \mathbf{B}.\tag{3}$$

Result 1: If $\mathbf{E_{exp,1}}$ is known for a given shorting factor value $s_{f,\,exp\,1}$, one can deduce the experimental value $\mathbf{E_{exp,2}}$ for any other shorting factor value $s_{f,\,exp\,2}$, provided that the spacecraft velocity $\mathbf{V_{sc}}$ and the ambient magnetic field $\mathbf{B}$ are known.

Proof 1: The relationship between $\mathbf{E_{exp,1}}$, $\mathbf{E_{exp,2}}$, and $\mathbf{V_{sc}} \times \mathbf{B}$ can be found by combining equations (2) and (3).

$$\mathbf{E_{exp,2}} = \frac{s_{f,\,exp2}}{s_{f,\,exp1}} \left(\mathbf{E_{exp,1}} + \mathbf{V_{sc}} \times \mathbf{B}\right) - \mathbf{V_{sc}} \times \mathbf{B}.\tag{4}$$

Thus,

$$\mathbf{E_{exp,2}} = \frac{s_{f,\,exp2}}{s_{f,\,exp1}}\mathbf{E_{exp,1}} + \left(\frac{s_{f,\,exp2} - s_{f,\,exp1}}{s_{f,\,exp1}}\right)\mathbf{V_{sc}} \times \mathbf{B}.\tag{5}$$

Reformulated in terms of electric drift $\mathbf{V_x} = (\mathbf{E_x} \times \mathbf{B})/B^2$, the equation (5) becomes

$$\mathbf{V_{exp,2}} = \frac{s_{f,\,exp2}}{s_{f,\,exp1}}\mathbf{V_{exp,1}} + \left(\frac{s_{f,\,exp1} - s_{f,\,exp2}}{s_{f,\,exp1}}\right)\mathbf{V_{sc,\perp}},\tag{6}$$

where $\mathbf{V_{sc,\perp}} = \mathbf{V_{sc}} - (\mathbf{V_{sc}} \cdot \mathbf{B})\mathbf{B}/B^2$ corresponds to the spacecraft velocity perpendicular to the magnetic field direction.

The objective is then to find the optimal value for the shorting factor so that the experimental electric field obtained is the true geophysical electric field of interest: $\mathbf{E_{exp}} = \mathbf{E_i}$.

2.3. The Difference Between the Experimental Estimate of the Geophysical Electric Field and the True Geophysical Electric Field Depends on the Difference Between the Shorting Factor Set by the Experimenter and the Shorting Factor True Value

Result 2: The experimental electric field $\mathbf{E_{exp}}$ equals the true geophysical electric field of interest $\mathbf{E_i}$ if and only if the shorting factor is equal to its appropriate value ($s_{f,exp} = s_{f,i}$). The difference between the experimental electric field $\mathbf{E_{exp}}$ and the true electric field of interest $\mathbf{E_i}$ depends on (a) the difference between the shorting factor set by the experimenter and the true shorting factor and (b) the amplitude of the spacecraft velocity perpendicular to magnetic field direction at the time of measurement.

Proof 2: Combining equations (1) and (2), one obtains that

$$\mathbf{E_{exp}} = \left(\frac{s_{f,\,exp}}{s_{f,i}}\right)\mathbf{E_i} + \left(\frac{s_{f,\,exp} - s_{f,i}}{s_{f,i}}\right)\mathbf{V_{sc}} \times \mathbf{B}.\tag{7}$$

In terms of electric drift, the equation (7) becomes

$$\mathbf{V_{exp}} = \left(\frac{s_{f,exp}}{s_{f,i}}\right)\mathbf{V_i} + \left(\frac{s_{f,i}-s_{f,exp}}{s_{f,i}}\right)\mathbf{V_{sc,\perp}}. \tag{8}$$

2.4. Conservation by Change of Reference Frame and Projection to the Magnetic Equator

Both results provided by equations (6) and (8) can be transposed to the corotating frame of reference. This is done by subtracting the corotation velocity perpendicular to the magnetic field direction $\mathbf{U_\perp}$ to both sides of the equal sign. For instance, with equation (8), we obtain that

$$\mathbf{V_{exp}} - \mathbf{U_\perp} = \left(\frac{s_{f,exp}}{s_{f,i}}\right)\mathbf{V_i} + \left(\frac{s_{f,i}-s_{f,exp}}{s_{f,i}}\right)\mathbf{V_{sc,\perp}} - \left(\frac{s_{f,i}-s_{f,exp}+s_{f,exp}}{s_{f,i}}\right)\mathbf{U_\perp}, \tag{9}$$

where $\mathbf{U_\perp} = (\mathbf{\Omega_E} \times \mathbf{r}) - ((\mathbf{\Omega_E} \times \mathbf{r}) \cdot \mathbf{B})\mathbf{B}/B^2$ is the projection of the corotational motion $\mathbf{\Omega_E} \times \mathbf{r}$ in a direction perpendicular to the magnetic field $\mathbf{B}$ at the location $\mathbf{r}$, and $\mathbf{\Omega_E}$ is the Earth's rotation vector. Thus,

$$\left(\mathbf{V_{exp}} - \mathbf{U_\perp}\right) = \left(\frac{s_{f,exp}}{s_{f,i}}\right)\left(\mathbf{V_i} - \mathbf{U_\perp}\right) + \left(\frac{s_{f,i}-s_{f,exp}}{s_{f,i}}\right)\left(\mathbf{V_{sc,\perp}} - \mathbf{U_\perp}\right). \tag{10}$$

With $\boldsymbol{\omega_x} = \mathbf{V_x} - \mathbf{U_\perp}$ the velocities in the corotating frame of reference, we obtain that

$$\boldsymbol{\omega_{exp}} = \left(\frac{s_{f,exp}}{s_{f,i}}\right)\boldsymbol{\omega_i} + \left(\frac{s_{f,i}-s_{f,exp}}{s_{f,i}}\right)\boldsymbol{\omega_{sc,\perp}}. \tag{11}$$

This vector relationship can be projected in both radial and azimuthal directions in the plane perpendicular to the magnetic field direction. These equations can also be projected to the magnetic equator assuming equipotential field lines. Let us define $\mathbf{W_x}$ the electric drift at the minimum-B locus of the equipotential field line that intersects spacecraft location. In the following, we show that there is a proportional relationship between $\mathbf{W_i}$ and $\boldsymbol{\omega_i}$. Thus,

$$\mathbf{W_{exp}} = \left(\frac{s_{f,exp}}{s_{f,i}}\right)\mathbf{W_i} + \left(\frac{s_{f,i}-s_{f,exp}}{s_{f,i}}\right)\mathbf{W_{sc,\perp}}. \tag{12}$$

Proof: With $\omega_{i,\rho}$ and $\omega_{i,\varphi}$ the radial and the azimuthal components of the geophysical electric drift $\boldsymbol{\omega_i}$ at spacecraft location and $W_{i,\rho}$ and $W_{i,\varphi}$ the radial and the azimuthal components of the geophysical electric drift projected at the minimum-B locus of the same equipotential field line $\mathbf{W_i}$, and we have indeed that

$$\begin{aligned} W_{i,\rho} &= R\omega_{i,\rho} \\ W_{i,\varphi} &= F\omega_{i,\varphi} \end{aligned}, \tag{13}$$

where R and F are amplification factors. These proportional relationships can be derived applying Faraday's law on closed infinitesimal loops connecting spacecraft location and magnetic equator (Lejosne & Mozer, 2016a, 2016b; Mozer, 1970). In the case of a dipole magnetic field,

$$\begin{aligned} R &= \frac{\sqrt{1+3\cos^2\theta}}{\sin^3\theta}, \\ F &= \frac{1}{\sin^3\theta} \end{aligned} \tag{14}$$

where θ is the magnetic colatitude of the measurement. The amplification factors of F and R are between 1 and 1.5 for magnetic latitudes between $-20°$ and $+20°$. In the most general case, R and F can be computed numerically assuming any numerical magnetic field model.

Thus, equation (12) is obtained by multiplying both sides of the vector relationship equation (11) by the 2×2 matrix $\boldsymbol{M} = \begin{bmatrix} R & 0 \\ 0 & F \end{bmatrix}$:
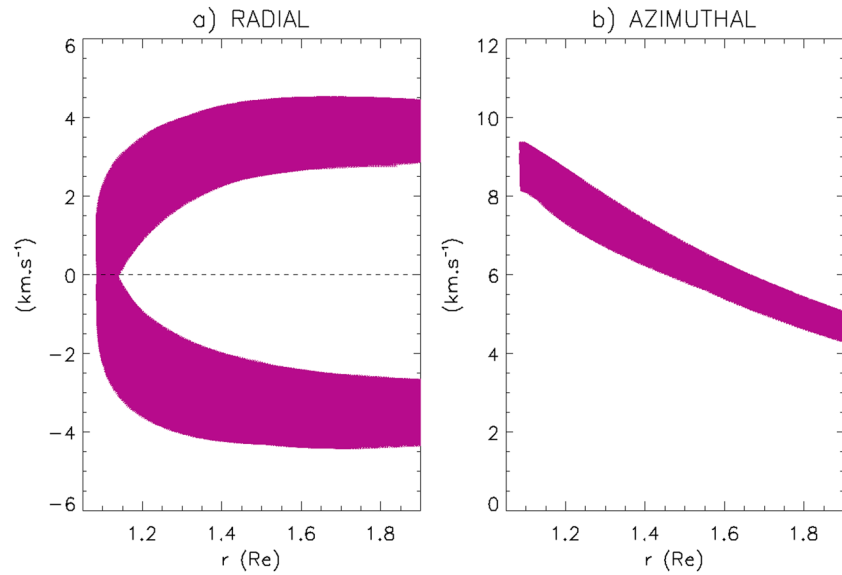
Figure 1. Van Allen Probe A velocity $\boldsymbol{\omega}_{\mathbf{sc},\perp}$ between October 2012 and December 2014, in both (a) radial and (b) azimuthal directions, as a function of spacecraft location ($r = \sqrt{x^2 + y^2 + z^2}$, where (x,y,z) corresponds to Geocentric Solar Ecliptic coordinates in units of Earth radii (Re)).

$$M \begin{bmatrix} \omega_{\exp,\rho} \\ \omega_{\exp,\varphi} \end{bmatrix} = \left(\frac{s_{f,\exp}}{s_{f,i}} \right) M \begin{bmatrix} \omega_{i,\rho} \\ \omega_{i,\varphi} \end{bmatrix} + \left(\frac{s_{f,i} - s_{f,\exp}}{s_{f,i}} \right) M \begin{bmatrix} \omega_{\mathbf{sc},\perp,\rho} \\ \omega_{\mathbf{sc},\perp,\varphi} \end{bmatrix}. \tag{15}$$

2.5. First Quantification of the Margins of Error Based on Van Allen Probes Ephemeris

Figure 1 represents the spacecraft velocity $\boldsymbol{\omega}_{\mathbf{sc},\perp}$ in the plane perpendicular to the magnetic field direction in the corotating frame of reference in both (a) radial and (b) azimuthal directions near perigee. The radial component of $\boldsymbol{\omega}_{\mathbf{sc},\perp}$ ranges between -4 and $+4$ km/s below $L = 2$. It is negative during inbound passes and positive during outbound passes. The azimuthal component of $\boldsymbol{\omega}_{\mathbf{sc},\perp}$ is always positive (i.e., eastward), and it is of the order of 5 to 10 km/s. This magnitude is about 10 to 100 times greater than the natural deviations from corotation for the geophysical field of interest $\boldsymbol{\omega}_{\mathbf{i}}$ (typically of the order of 10^{-2} to 10^{-1} km/s; e.g., Richmond et al., 1980; see also Lejosne & Mozer, 2016a). Thus, according to equation (11), any small inaccuracy in the value set for the shorting factor can lead to significant inaccuracies in the resulting $\boldsymbol{\omega}_{\mathbf{exp}}$.

For instance, let us assume 10% of error in the value of the shorting factor: $s_{f,i} = 1$, while the experimenter chooses to set $s_{f,\exp} = 1.1$. With $\omega_{i,\varphi} = 0.1$ km/s and $\omega_{sc, \perp, \varphi} = 5$ km/s, one obtains from equation (11) that $\omega_{\exp} \cong 0.6$ km/s and $\omega_{\exp}/\omega_i \cong 6$. Therefore, even a small error for the shorting factor value has a serious impact on the accuracy of the geophysical electric field measurements.

3. Method to Determine the Amplitude of the Shorting Factor for the Van Allen Probes Near Perigee DC Electric Field Measurements

3.1. Database of Electric Drift Measurements

The electric drift database corresponds to spin-averaged (~12 s) magnetic (Kletzing et al., 2013) and electric (Wygant et al., 2013) field measurements collected by Van Allen Probes A and B between 1 October 2012 and 31 December 2014. This time interval corresponds to the prime phase of the mission, that is, a time during which the best quality measurements were recorded in a sufficient number to carry the proposed analysis. The Van Allen Probes have an apogee at 5.8 Earth radii, a perigee around 1,000 km, a period of 9 hr, and an inclination of 10°. Spacecraft apogees drift slowly so that it takes a bit less than 2 years to scan all local time sectors.

To obtain reliable electric drift measurements, a slight (<1°) misalignment in the magnetometer axes for both spacecraft was corrected (Lejosne & Mozer, 2016a). In addition, the data from the short-axis electric
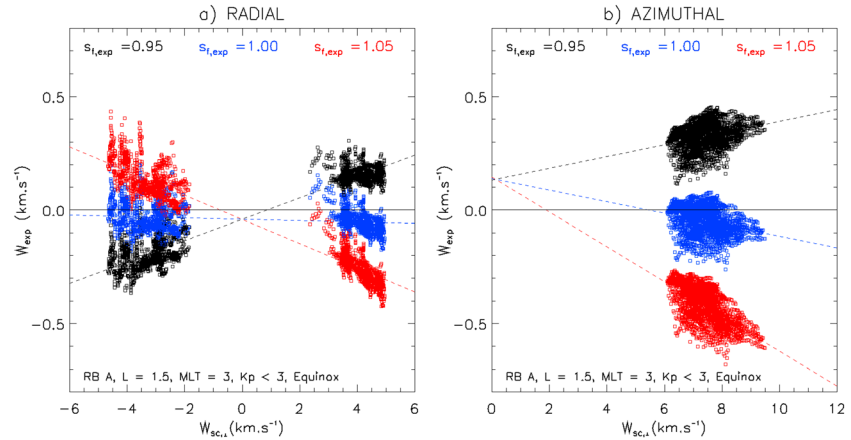
Figure 2. (a) Radial and (b) azimuthal components of the experimental estimates for the natural deviation from corotation at magnetic equator $\mathbf{W_{exp}}$ for a shorting factor set to 0.95 (black), 1.00 (blue), and 1.05 (red) based on Van Allen Probes A direct-current electric field measurements. The data are represented as a function of spacecraft velocity $\mathbf{W_{sc,\perp}}$. To reduce the natural variations of the quantity estimated ($\mathbf{W_i}$), the database is restricted to measurements during equinox and quiet times (Kp < 3), at a given location: L = 1.5 ($\pm$0.1) and MLT = 3 hr ($\pm$0.5). The dashes lines represent the results of the least squares linear regression performed for each component and each shorting factor value.

field antenna were replaced by the assumption that the parallel electric field is zero, because of the plasma's high conductivity parallel to magnetic field lines. Measurements collected during or just after spacecraft maneuvers were discarded. When processing the database, we assumed that the boom length was accurately known ($s_{f,exp} = 1$).
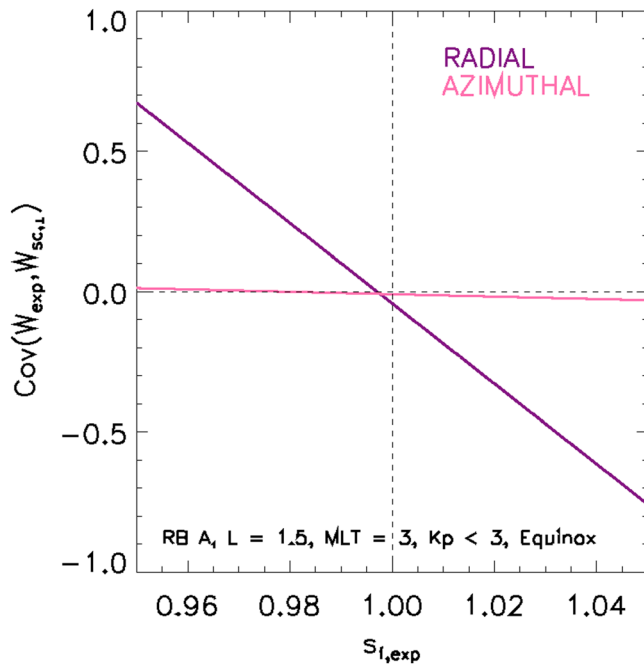

Figure 3. Covariance between the empirical estimates for the geophysical electric drift $\mathbf{W_{exp}}$ and the spacecraft velocities $\mathbf{W_{sc,\perp}}$, computed independently in both radial (purple) and azimuthal (pink) directions, as a function of the value set by the experimenter for the shorting factor $s_{f,exp}$. The data set used for this plot is the same as Figure 2 (i.e., Van Allen Probes A measurements during equinox and quiet times [Kp < 3], around a fixed L and MLT: L = 1.5 [$\pm$0.1] and MLT = 3 hr [$\pm$0.5]).

The different estimates for the geophysical electric field (obtained assuming different values for the shorting factor $s_{f,exp}$) were deduced from the combination of database values ($s_{f,exp} = 1$) and spacecraft velocities (following equation (6)). In the remainder, the measurements discussed are in the Earth's corotating frame of reference and after projection to the magnetic equator assuming equipotential field lines.

3.2. Illustration to Introduce the Method for In-Flight Calibration of the Shorting Factor Near Perigee

Figure 2 presents experimental estimations of the natural deviation from corotation, in both radial (Figure 2a) and azimuthal (Figure 2b) directions, based on Van Allen Probes A DC electric field measurements. The different estimates are presented for different experimental values of the shorting factor ($s_{f,exp} = [0.95; 1.00; 1.05]$). To reduce the variability of the quantity estimated ($\mathbf{W_i}$), we restricted the database to measurements during quiet geomagnetic times (Kp < 3), at equinox, around L = 1.5 ($\pm$0.1) and MLT = 3 hr ($\pm$0.5). For each component and for each shorting factor, a linear least square interpolation was performed. Each linear fit is represented by a dashed line in Figure 2.

For each of the three values assumed for the shorting factor ($s_{f,exp} = [0.95; 1.00; 1.05]$), there is a correlation between the spacecraft velocity $\mathbf{W_{sc,\perp}}$ and the experimental estimates for the natural deviation from corotation at magnetic equator $\mathbf{W_{exp}}$. For $s_{f,exp} = 0.95$, the correlation is positive (the slopes of the linear fits are positive for $s_{f,exp} = 0.95$, Figure 2, with a value of 0.0471 ± 0.0003 in the radial direction and 0.026 ± 0.002 in the azimuthal direction). For $s_{f,exp} = 1.00$ and $s_{f,exp} = 1.05$, the correlation is negative (the slopes of the linear fits are negative Figure 2). For $s_{f,exp} = 1.00$, they are equal to -0.0030 ± 0.0003 in the radial direction and
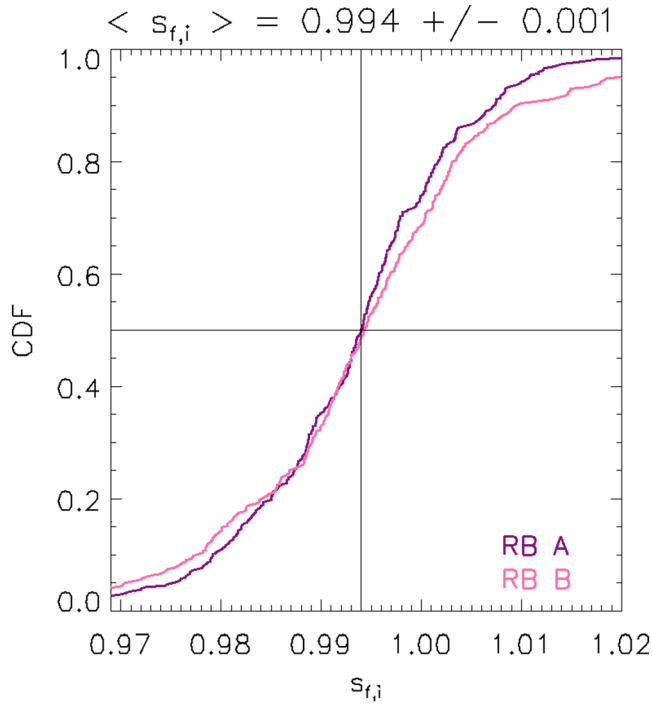
Figure 4. Cumulative distribution function (CDF) for the appropriate value of the shorting factor $s_{f,i}$ for Van Allen Probes A (RB A, in purple) and Van Allen Probes B (RB B, in pink). The median value for $s_{f,i}$ is 0.994, and the standard error of the mean is of 0.001.

-0.025 ± 0.002 in the azimuthal direction. For $s_{f,exp} = 1.05$, they are equal to -0.0532 ± 0.0003 in the radial direction and -0.077 ± 0.002 in the azimuthal direction. This correlation between $\mathbf{W_{sc,\perp}}$ and $\mathbf{W_{exp}}$ provides information on the appropriate value for the shorting factor $s_{f,i}$. If $s_{f,i} \ll s_{f,exp}$, we have indeed that $\mathbf{W_{exp}} = -(s_{f,exp}/s_{f,i})(\mathbf{W_{sc,\perp}} - \mathbf{W_i}) \sim -(s_{f,exp}/s_{f,i})\mathbf{W_{sc,\perp}}$ (equation (12)). Thus, $\mathbf{W_{exp}}$ is negatively correlated to $\mathbf{W_{sc,\perp}}$ when $s_{f,exp}$ is greater than $s_{f,i}$. Similarly, if $s_{f,i} \gg s_{f,exp}$, $\mathbf{W_{exp}} \sim \mathbf{W_{sc,\perp}}$. $\mathbf{W_{exp}}$ is positively correlated to $\mathbf{W_{sc,\perp}}$ when $s_{f,exp}$ is smaller than $s_{f,i}$. When $s_{f,exp} = s_{f,i}$, $\mathbf{W_{exp}} = \mathbf{W_i}$. The variable $\mathbf{W_i}$ corresponds to geophysical deviations from corotation. These deviations are occurring naturally. They do not depend on spacecraft velocity. In other words, $\mathbf{W_i}$ and $\mathbf{W_{sc,\perp}}$ are statistically independent variables. Therefore, when $s_{f,exp} = s_{f,i}$, the covariance (and thus the correlation) between $\mathbf{W_{exp}} = \mathbf{W_i}$ and $\mathbf{W_{sc,\perp}}$ should be 0.

With that in mind, we deduce from Figure 2 that

1. $0.95 < s_{f,i} < 1.00$ (because the correlation between $\mathbf{W_{exp}}$ and $\mathbf{W_{sc,\perp}}$ is positive for $s_{f,exp} = 0.95$, we have $0.95 < s_{f,i}$; and because the correlation is negative for $s_{f,exp} = 1.00$, we have $s_{f,i} < 1$); and
2. $s_{f,i}$ is closer to 1.00 than to 0.95 (because the amplitude of the correlation between $\mathbf{W_{exp}}$ and $\mathbf{W_{sc,\perp}}$ is greater for $s_{f,exp} = 0.95$ than for $s_{f,exp} = 1.00$).

Using the same subset of the database, we computed the covariance between the variables $\mathbf{W_{exp}}$ and $\mathbf{W_{sc,\perp}}$ as a function of the value set by the experimenter for the shorting factor $s_{f,exp}$. The results are presented Figure 3.

Figure 3 extends the results from Figure 2. For $s_{f,exp} = 0.95$, the covariance is positive, while for $s_{f,exp} = 1.00$ and $s_{f,exp} = 1.05$, the covariance is negative. In addition, the covariance cancels in the neighborhood of 1^- (i.e., it is zero for a value that is smaller than 1 but close to 1). So the appropriate setting for the shorting factor is in the neighborhood of 1^-.

The covariance cancels for slightly different values when we compare the results in the radial direction and in the azimuthal direction. Yet we note that the covariance varies more dramatically with $s_{f,exp}$ in the radial direction than in the azimuthal direction. This is because the spacecraft velocity varies on a wider range in the radial direction than in the azimuthal direction. (Because the spacecraft crossed the same (L,MLT) bin during both inbound and outbound passes, the variance for the spacecraft velocity is greater in the radial direction than in the azimuthal direction. See also Figure 1.) Therefore, it is more accurate to analyze the covariance between $\mathbf{W_{exp}}$ and $\mathbf{W_{sc,\perp}}$ in the radial direction than in the azimuthal direction to calibrate the shorting factor.

3.3. Results

We extended the method described section 3.2 to a variety of subsets of the database. We analyzed 400 different (L,MLT) bins, covering the entire region below $L = 2$, for different levels of magnetic activities ($Kp < 3$ or $Kp \geq 3$) and for different seasons. For each subset, we recorded the value of the shorting factor that canceled the covariance between $\mathbf{W_{exp}}$ and $\mathbf{W_{sc,\perp}}$ in the radial direction. For each scenario, we obtained a slightly different value for $s_{f,i}$. (This is because the data have different noise levels, they are measured under different magnetic activity conditions, etc.) We ordered all the possible values obtained for $s_{f,i}$, and we generated a cumulative distribution function. The results are presented Figure 4 for both Van Allen Probes A and B.

The median value for the shorting factor is 0.994, and the standard error of the mean is of 0.001 for both Van Allen Probes. Assuming that $s_{f,i}$ is a constant in the plasmasphere, we obtain that $s_{f,i} = 0.994 \pm 0.001$. This margin of error corresponds to uncertainties that are smaller than 10 m/s in the resulting electric drift, according to equation (12). Because the spacecraft have higher velocities in the azimuthal direction than

in the radial direction (Figure 1), the margins of errors in individual electric drift measurements are greater in the azimuthal direction than in the radial direction. The margins of errors are approximately of the order of ± 3 m/s in the radial direction of the electric drift $(0.001 \times W_{sc,\perp} \cong 0.001 \times 3$ km/s) and ± 6 m/s in the azimuthal direction at L = 1.5.

In an independent analysis, we recorded the values of the shorting factor that would cancel the covariance between W_{exp} and $W_{sc,\perp}$ in the azimuthal direction (rather than in the radial direction). We obtained the same resulting median value for the shorting factor, but the resulting standard errors were two times greater. This confirms the idea that the method proposed is most accurate when the variance of the spacecraft velocity is the largest.

4. Conclusion

In this article, we have provided theoretical results in order to assess the effects of shorting factor uncertainties when measuring geophysical DC electric fields near perigee. We have developed a method to derive the shorting factor based on the idea that spacecraft velocity and geophysical electric drift are statistically independent variables. The main advantage of this approach is that it does not require theoretical preconceptions about the dynamics of the geophysical electric drift. For Van Allen Probes measurements near perigee, we obtain a shorting factor that is very close to 1, as expected.

The shorting factor is composed of two components: (1) the shorting of the electric field by the conductors in the medium and (2) uncertainty in the length of the antenna. Below L = 2, the resultant measurement reflects more the uncertainty in the boom length than that it represents some phenomena in the plasma (because the Debye length is short enough that item 1 is 1 at any low L value). The uncertainty in the boom length due to the stretching of the wire by the centrifugal force, the uncertainty in the amount deployed, and so forth easily accounts for the fact that the shorting factor differs from 1. This uncertainty does not depend on changes in the ambient environment. That is why a constant value is assumed for the shorting factor below L = 2.

The margin of uncertainty around the shorting factor value provides an estimate for the corresponding margin of error of the individual DC electric drift measurements. Due to the higher spacecraft velocity in the azimuthal direction, the margin of error for the individual DC electric drift measurements is about 2 times greater in the azimuthal direction than in the radial direction. Assuming that the only possible source of error for the electric drift measurements is an error in the value of the shorting factor, the amplitude of the margin of error obtained is remarkably small: of the order of a few meters per second only. A more detailed error budget requires the quantification of other factors of uncertainty in electric drift measurements (such as the uncertainty introduced by the assumption that the parallel electric field is zero, uncertainties in spacecraft velocity, and uncertainties in magnetic field direction).

References

Bonnell, J. W., Mozer, F. S., Delory, G. T., Hull, A. J., Ergun, R. E., Cully, C. M., et al. (2008). The Electric Field Instrument (EFI) for THEMIS. *Space Science Reviews*, *141*(1-4), 303–341. https://doi.org/10.1007/s11214-008-9469-2

Califf, S., & Cully, C. M. (2016). Empirical estimates and theoretical predictions of the shorting factor for the THEMIS double-probe electric field instrument. *Journal of Geophysical Research: Space Physics*, *120*, 6223–6233. https://doi.org/10.1002/2016JA022589

Cully, C. M., Ergun, R. E., & Eriksson, A. I. (2007). Electrostatic structure around spacecraft in tenuous plasmas. *Journal of Geophysical Research*, *112*, A09211. https://doi.org/10.1029/2007JA012269

Engwall, E., Eriksson, A. I., & Forest, J. (2006). Wake formation behind positively charged spacecraft in flowing tenuous plasmas. *Physics of Plasmas*, *13*(6), 062904. https://doi.org/10.1063/1.2199207

Ergun, R. E., Carlson, C. W., Mozer, F. S., Delory, G. T., Temerin, M., McFadden, J. P., et al. (2001). The FAST satellite fields instrument. *Space Science Reviews*, *98*(1/2), 67–91. https://doi.org/10.1023/A:1013131708323

Fahleson, U. (1967). Theory of electric field measurements conducted in the magnetosphere with electric probes. *Space Science Reviews*, *7*(2-3), 238–262. https://doi.org/10.1007/BF00215600

Gustafsson, G., Boström, R., Holback, B., Holmgren, G., Lundgren, A., Stasiewicz, K., et al. (1997). The electric field and wave experiment for the Cluster Mission. *Space Science Reviews*, *79*(1/2), 137–156. https://doi.org/10.1023/A:1004975108657

Khotyaintsev, Y. V., Lindqvist, P.-A., Cully, C. M., Eriksson, A. I., & Andre, M. (2014). In flight calibration of double-probe electric field measurements on Cluster. *Geoscientific Instrumentation, Methods and Data Systems*, *3*(2), 143–151. https://doi.org/10.5194/gi-3-143-2014

Kletzing, C. A., Kurth, W. S., Acuna, M., MacDowall, R. J., Torbert, R. B., Averkamp, T., et al. (2013). The Electric and Magnetic Field Instrument Suite and Integrated Science (EMFISIS) on RBSP. *Space Science Reviews*, *179*(1-4), 127–181.

Lejosne, S., & Mozer, F. S. (2016a). Van Allen Probe measurements of the electric drift E × B/B2 at Arecibo's L = 1.4 field line coordinate. *Geophysical Research Letters*, *43*, 6768–6774. https://doi.org/10.1002/2016GL069875

Lejosne, S., & Mozer, F. S. (2016b). Typical values of the electric drift E × B/B2 in the inner radiation belt and slot region as determined from Van Allen Probe measurements. *Journal of Geophysical Research: Space Physics*, *121*, 12,014–12,024. https://doi.org/10.1002/2016JA023613

Lindqvist, P. A., Olsson, G., Torbert, R. B., King, B., Granoff, M., Rau, D., et al. (2016). The spin-plane double probe electric field instrument for MMS. *Space Science Reviews*, *199*(1-4), 137–165. https://doi.org/10.1007/s11214-014-0116-9

Mozer, F. S. (1970). Electric field mapping in the ionosphere at the equatorial plane. *Planetary and Space Science*, *18*(2), 259–263. https://doi.org/10.1016/0032-0633(70)90161-3

Mozer, F. S. (2016). DC and low-frequency double probe electric field measurements in space. *Journal of Geophysical Research: Space Physics*, *121*, 10,942–10,953. https://doi.org/10.1002/2016JA022952

Mozer, F. S., Carlson, C. W., Hudson, M. K., Torbert, R. B., Parady, B., Yatteau, J., & Kelley, M. C. (1977). Observations of paired electro-static shocks in the polar magnetosphere. *Physical Review Letters*, *38*(6), 292–295. https://doi.org/10.1103/PhysRevLett.38.292

Mozer, F. S., Torbert, R. B., Fahleson, U. V., Falthammar, C. G., Gonfalone, A., & Pedersen, A. (1978). Measurements of quasi-static and low-frequency electric fields with spherical double probes on the ISEE-1 spacecraft. *IEEE Transactions on Geoscience Electronics*, *16*(3), 258–261. https://doi.org/10.1109/TGE.1978.294558

Pedersen, A., Cattell, C. A., Falthammar, C.-G., Formisano, V., Lindqvist, P.-A., Mozer, F., & Torbert, R. (1984). Quasistatic electric field measurements with spherical double probes on the GEOS and ISEE satellites. *Space Science Reviews*, *37*, 269–312.

Pedersen, A., Mozer, F., & Gustafsson, G. (1998). Electric field measurements in a tenuous plasma with spherical double probes. In R. F. Pfaff, J. E. Borovsky, & D. T. Young (Eds.), *Measurement techniques in space plasmas fields*, *Geophysical Monograph Series* (Vol. 103, pp. 1–12). Washington, DC: American Geophysical Union. https://doi.org/10.1002/9781118664391

Richmond, A. D., Blanc, M., Emery, B. A., Wand, R. H., Fejer, B. G., Woodman, R. F., et al. (1980). An empirical model of quiet-day ionospheric electric fields at middle and low latitudes. *Journal of Geophysical Research*, *85*(A9), 4658–4664. https://doi.org/10.1029/JA085iA09p04658

Wygant, J. R., Bonnell, J. W., Goetz, K., Ergun, R. E., Mozer, F. S., Bale, S. D., et al. (2013). The electric field and wave instruments on the Radiation Belt Storm Probes mission. *Space Science Reviews*, *179*(1-4), 183–220. https://doi.org/10.1007/s11214-013-0013-7

Wygant, J. R., Harvey, P. R., Pankow, D., Mozer, F. S., Maynard, N., Singer, H., et al. (1992). CRRES electric field/Langmuir probe instrument. *Journal of Spacecraft and Rockets*, *29*(4), 601–604. https://doi.org/10.2514/3.25507